arXiv:1701.07648v1 [cond-mat.mtrl-sci] 26 Jan 2017

Microscopic Aspects of Magnetic Lattice Demagnetizing Factors

M. Twengström,[1] L. Bovo,[2] M. J. P. Gingras,[3,4,5] S. T. Bramwell,[2] and P. Henelius[1]

[1] *Department of Physics, Royal Institute of Technology, SE-106 91 Stockholm, Sweden*
[2] *London Centre for Nanotechnology and Department of Physics and Astronomy, University College London, 17-19 Gordon Street, London, WC1H OAH, U.K.*
[3] *Department of Physics and Astronomy, University of Waterloo, Waterloo, Ontario, N2L 3G1, Canada*
[4] *Canadian Institute for Advanced Research, 180 Dundas St. W., Toronto, Ontario, M5G 1Z8, Canada*
[5] *Perimeter Institute for Theoretical Physics, 31 Caroline St. N., Waterloo, Ontario, N2L 2Y5, Canada*

Considering localized magnetic moments on a lattice, we show that the demagnetizing factor for a non-ellipsoidal sample depends on the spin dimensionality (Ising, XY or Heisenberg) and orientation, as well as the sample shape and susceptibility. Our result indicates that the common practice of approximating the true sample shape with ellipsoids for systems with long-range interactions may, in certain cases, overlook important effects stemming from the *microscopic* aspects of the system.

Long-range interactions are fundamentally important in many areas of science, from cosmology, through the gravitational interaction, to biology, through Coulomb's law. A long-range interaction may be defined in d spatial dimensions by its two-body potential $V(r)$ scaling with distance r as $r^{-\alpha}$ where $\alpha \leq d$ [1]. The paramount problem in such systems is how to integrate $V(r)$ over an extended system. Following Newton and Euler, the analysis of general systems has been largely based on the exact solutions for spheres and ellipsoids [2–6]. This raises the question of whether approximating other shapes to ellipsoids just neglects uninteresting details or *whether there are crucial properties that are lost in the approximation*. The demagnetizing problem in magnetic systems is a natural setting for exploring this question since it is accessible and of intrinsic importance in experiments, and constitutes a paragon for the exploration of the thermodynamics of systems with long-range interactions [1]. Demagnetizing factors are also crucial in the experimental investigation of superconducting systems. Analogues occur in electrical systems [7] (the depolarization factor), in the problem of strain fields around inclusions [8], and in the treatment of avalanching systems in confined geometries [9–11], just to name a few.

In an applied magnetic field, the thermodynamic energy of an ellipsoidal magnetic sample acquires a magnetostatic contribution $E_{\rm mag} = (\mu_0/2)Nm^2/V$, where N is the demagnetizing factor, V is the volume and m the magnetic moment. After subtracting $E_{\rm mag}$ from the total energy, differentiation of the corrected energy amounts to an effective *reduction* of the applied field, $B_{\rm ext}$, by $\mu_0 NM$, where $M \equiv m/V$ is the magnetization. Viewed as a correction to $H_{\rm ext} \equiv B_{\rm ext}/\mu_0$, this is the demagnetizing field $H_{\rm d} = -NM$ within the sample. With an internal field $H_{\rm int} \equiv H_{\rm ext} + H_{\rm d}$, one finds an *intrinsic* magnetic susceptibility $\chi_{\rm int} = \partial M/\partial H_{\rm int}$, a *shape-independent material property*, which relates to the experimentally determined susceptibility, $\chi_{\rm exp} \equiv \partial M/\partial H_{\rm ext}$, through

$$\frac{1}{\chi_{\rm int}} = \frac{1}{\chi_{\rm exp}} - N. \qquad (1)$$

The determination of N is a fundamental problem and dates back to the work of Poisson and Maxwell [12]. In the 1940s, Osborn [2] and Stoner [3] tabulated N for general ellipsoids, while more recently, Aharoni [13] treated cuboids in the $\chi_{\rm int} \to 0$ limit. These highly cited papers bear witness to the importance of accurately computable and easily accessible demagnetizing factors. Given that *i)* it was realized already in the 1920s that N for a non-ellipsoidal sample is a function not only of the sample shape, but also of $\chi_{\rm int}$ itself [14, 15] and that *ii)* many experiments are routinely performed not on ellipsoids, but on cuboids [16, 17], it is perhaps remarkable that it was only very recently that the χ-dependence of N was calculated for cuboids away from the $\chi_{\rm int} \to 0$ limit [18, 19].

The existence of demagnetizing factors for cuboids suggests that their thermodynamics may be formulated in terms of an internal field, with corrections that become dependent on both shape and temperature [18] (through $\chi_{\rm int}$). In this work we have found that, for magnetic lattices, the demagnetizing factor of cuboids depends *also* on the local symmetry and allowed orientations of the magnetic moments. With reference to the question posed at the very beginning, our result illustrates a case where a long-range interaction integrates in a qualitatively different way for a cuboid and an ellipsoid, such that the discrete microscopic nature of the system matters in the former case but not in the latter. We are aware of only a few previous studies where effects of such discreteness have been discussed [7, 20–22]. In particular, Millev *et al.* [22] found a multiplicative separation of discrete and continuum contributions to the demagnetizing effects for systems with restricted geometries. In our work, we demonstrate discreteness effects *even* in the $3d$ thermodynamic limit. Our interest in this problem was partly spurred by the perplexing recent experimental observation of anomalous demagnetizing effects in the spin ice material $Dy_2Ti_2O_7$ [23].

One may ask whether small differences in estimated demagnetizing factors really matter for exposing important and interesting physics. The answer is found in Eq. (1). If $\chi_{\rm exp}$, and N are both small, then this transforma-

tion does not renormalize the sought $\chi_{\rm int}$ appreciably, being rather insensitive to the precise value of N. However, in many physical systems displaying unusual magnetic phenomena, $\chi_{\rm exp}$ can be large, and $\chi_{\rm int}$ is, through Eq. (1), a highly sensitive function of N. Examples include the rare-earth based spin ice materials $Dy_2Ti_2O_7$ and $Ho_2Ti_2O_7$, which support magnetic monopole excitations [24], and $LiHo_{1-x}Y_xF_4$ which displays ultraslow relaxational behavior [25]. Important demagnetizing effects are manifest in experiments requiring an accurately directed external field, as in the case of the elusive Kasteleyn transition [26], sub-lattice pinning [17, 27–29], or multiple field-driven transitions [30], or disentangling the in-phase and out-of-phase response for non-zero frequency stimuli [31]. In order to reach quantitative conclusions from the deduced $\chi_{\rm int}$, or to accurately test theoretical predictions, it is necessary to determine N highly accurately. Our work illustrates that one may indeed achieve this (see Fig 1).

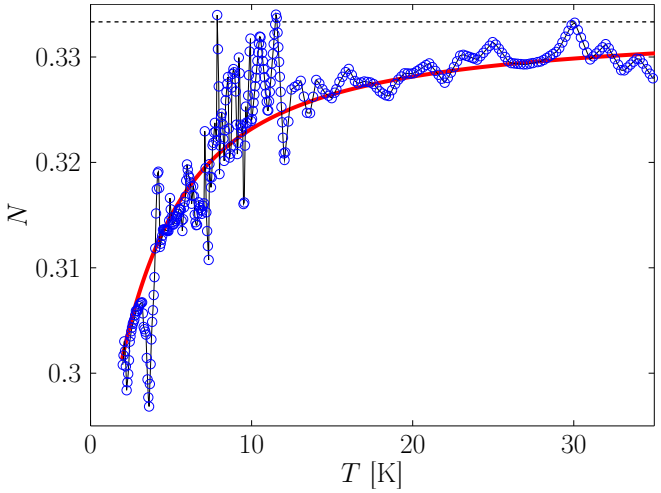

FIG. 1. N as a function of T for a cubic sample of the spin ice $Dy_2Ti_2O_7$. Shown are experimental results (blue open circles) and our fitting parameter-free theory (red line). The dashed reference line shows the exact $N = 1/3$ value for a sphere [2]

Determination of N via an iterative method – In the spirit of problems (6.18) and (4.23) in Griffiths [32], we use an iterative method to calculate the on-site field distribution inside a linear magnetic material placed in a uniform magnetic field. Initially, we assume that $H_{\rm int}$ equals $H_{\rm ext}$ and calculate the induced local magnetization for an assumed $\chi_{\rm int}$. This magnetization generates a demagnetizing field that, in turn, modifies $H_{\rm int}$. The resulting field-magnetization equations are iterated until convergence. With the converged field and magnetization distributions in hand, one then computes N.

To proceed, we consider a sample of volume V with $\mathcal{N}$ magnetic moments. Initially, we focus on Ising moments $\boldsymbol{m}_i = m_i\mu_B\hat{\mathbf{i}}$, where $\hat{\mathbf{i}}$ is the unit vector in the local Ising direction at site i, and m_i is dimensionless. We first determine the component of the local field along the Ising moment at site i, $B_i^{\shortparallel} = \boldsymbol{B}_i \cdot \hat{\mathbf{i}}$, which is the sum of three contributions:

$$B_i^{\shortparallel} = B_i^{\shortparallel,\rm dip} + B_i^{\shortparallel,\rm ext} + B_i^{\shortparallel,\rm self}, \tag{2}$$

which we discuss one by one.

First, the dipolar field at site i produced by *all the other* point magnetic dipoles within the sample, $B_i^{\shortparallel,\rm dip} \equiv \boldsymbol{B}_i^{\rm dip} \cdot \hat{\mathbf{i}}$, is given by the familiar form [32]

$$B_i^{\shortparallel,\rm dip} = \frac{\mu_0\mu_{\rm B}}{4\pi} \sum_{j\neq i} \left(\frac{3(\hat{\mathbf{j}} \cdot \hat{\boldsymbol{r}}_{ij})(\hat{\mathbf{i}} \cdot \hat{\boldsymbol{r}}_{ij}) - \hat{\mathbf{j}} \cdot \hat{\mathbf{i}}}{r_{ij}^3} \right) m_j. \tag{3}$$

Second, we consider an external field in the $\hat{\boldsymbol{z}}$ direction, $\boldsymbol{B}_i^{\rm ext} = B^{\rm ext}\hat{\boldsymbol{z}}$, with $B_i^{\shortparallel,\rm ext} = B^{\rm ext}\cos\theta_i$, where $\cos\theta_i \equiv \hat{\boldsymbol{z}} \cdot \hat{\mathbf{i}}$, the angle between the direction of the Ising axis at site i and the direction of $\boldsymbol{B}_i^{\rm ext}$, $\hat{\boldsymbol{z}}$.

Third, is the contribution from the self-field, $B_i^{\shortparallel,\rm self}$. In the classic case of a single point dipole [32, 33], a term $\frac{2}{3}\mu_0\mu_{\rm B}\delta(\boldsymbol{r})$ must be added to ensure that the average magnetic field in a sphere containing the dipole gives the correct macroscopic field. Similarly, we add a self-field to ensure that the internal magnetic field in a uniformly magnetized sample results in the expected value, for example $\boldsymbol{B} = \frac{2}{3}\mu_0\boldsymbol{M}$ for a uniformly magnetized sphere or cube [19]. We are primarily concerned with paramagnetic samples in the linear response regime, where a weak magnetic field induces a magnetization proportional to it, as in a typical χ measurement. For a non-ellipsoidal sample, the induced magnetization will in general be non-uniform, except in the $\chi \to 0$ limit. In this limit, $H_{\rm d}$ vanishes and, as a consequence, $H_{\rm int}$ and M are uniform. Our goal is to determine the self-field so that the magnetic field has the expected value in the $\chi \to 0$ limit. We demonstrate the basic idea with two examples.

We first take a cubic sample with all moments aligned in the global $\hat{\boldsymbol{z}}$ direction. In this case $\boldsymbol{B}$, $\boldsymbol{M}$ and $\boldsymbol{H}$ are all aligned with the $\hat{\boldsymbol{z}}$ direction for which the field equation $\boldsymbol{B} = \mu_0(\boldsymbol{M} + \boldsymbol{H})$ reduces to $B^z = \mu_0(M^z - N_0M^z) = \frac{2}{3}\mu_0M^z$, where $N_0 = \frac{1}{3}$ is the $\chi \to 0$ limit of N for a cube [19]. If we consider a simple cubic lattice, it is well known that the lattice sum vanishes [34]. This implies that $B^{z,\rm self} = \frac{2}{3}\mu_0M^z$ must be incorporated to ensure the expected net field value.

Next, we consider the case of a lattice where the Ising axes are tilted by an angle θ with respect to the z-axis, and half the spins tilt to the right and half to the left so that there is no net magnetization in the $\hat{\boldsymbol{x}}$ or $\hat{\boldsymbol{y}}$ directions. The total $\boldsymbol{B}$, $\boldsymbol{M}$ and $\boldsymbol{H}$ fields are in the $\hat{\boldsymbol{z}}$-direction, but the question is what should the $B^{\shortparallel}$ field parallel to the magnetic moments be? From $\boldsymbol{B} = \mu_0(\boldsymbol{M} + \boldsymbol{H})$, it follows that $\boldsymbol{B}$ is generated by *two terms*, which we discuss separately. We begin with the term generated directly by $\boldsymbol{M}$, namely $\boldsymbol{B}^1 = \mu_0\boldsymbol{M}$, or

$B^{1,z} = \mu_0 M^z = \mu_0 M^{\shortparallel} \cos\theta$, where $M^{\shortparallel}$ is the magnetization in the local Ising directions, $M^{\shortparallel} = V^{-1} \sum_{i=1}^{\mathcal{N}} \boldsymbol{m}_i \cdot \hat{\mathbf{i}}$. This equation is satisfied by $B^{1,\shortparallel} = \mu_0 M^{\shortparallel}$. The second term, $B^{2,z} = \mu_0 H^z = -\mu_0 N_0 M^z = -\mu_0 N_0 M^{\shortparallel} \cos\theta$ is generated by $H_{\rm d}$. The field along the magnetic moment is $B^{2,\shortparallel} = -\mu_0 N_0 M^{\shortparallel} \cos^2\theta$, and the net self-field becomes

$$B_i^{\shortparallel,\rm self} = B^{1,\shortparallel} + B^{2,\shortparallel} = \mu_0 \mu_B \frac{\mathcal{N}}{V} \left[1 - N_0 \cos^2\theta\right] m_i, \quad (4)$$

which is valid when the dipolar lattice sum, Eq. (3), vanishes and when the average $\boldsymbol{M}$ is along $\boldsymbol{B}^{\rm ext}$. In case the lattice sum does not vanish, it must be subtracted from the self-field in order to ensure the expected net field value.

Eqs. (2, 3, 4) give the local field in terms of the set of local magnetizations, $\{m_i\}$. Next we "invert" this to get the $\{m_i\}$ induced by $B_i^{\shortparallel}$. Using $\boldsymbol{M} = \chi \boldsymbol{H}$ (linear media) we get $\boldsymbol{B} = \mu_0(\boldsymbol{M} + \boldsymbol{M}/\chi) = \mu_0 \frac{\chi+1}{\chi} \boldsymbol{M}$, or $\boldsymbol{M} = \frac{\chi}{\chi+1} \frac{\boldsymbol{B}}{\mu_0}$, leading to

$$m_i = \frac{V}{\mathcal{N}} \left(\frac{\chi_{\rm loc}}{\chi_{\rm loc} + 1}\right) \frac{B_i^{\shortparallel}}{\mu_0 \mu_B}, \quad (5)$$

where $\chi_{\rm loc}$ is the local susceptibility in the $\hat{\mathbf{i}}$ direction.

We can now iterate the expressions for $B_i^{\shortparallel}$ in Eq. (2) and m_i in Eq (5) until convergence, and then calculate N from Eq. (1), where $\chi_{\rm exp}$ is given by

$$\chi_{\rm exp} = \chi_{\rm exp}^{zz} = \left(\frac{\partial M^z}{\partial H_{\rm ext}^z}\right)_T = \frac{\mu_0 \mu_B}{V B^{\rm ext}} \sum_{i=1}^{\mathcal{N}} m_i \cos\theta. \quad (6)$$

The intrinsic susceptibility, $\chi_{\rm int}$, expresses the relation between $\boldsymbol{B}^{\rm ext}$ and induced $\boldsymbol{M}$ under so-called "Ewald", or "tin foil", boundary condition [35] which eliminates demagnetizing fields and corresponds to the $N = 0$ limit. As a result, both $\chi_{\rm int}$ and $\chi_{\rm loc}$ are responses to an *internal* field. While $\chi_{\rm int}$ measures the response in the direction of $H_{\rm ext}$, $\chi_{\rm loc}$ measures the response along the local Ising axis $\hat{\mathbf{i}}$. With $\hat{\boldsymbol{z}} \cdot \hat{\mathbf{i}} = \cos\theta$, $H_{\rm ext}^z \cos\theta$ induces a magnetization $M^{\shortparallel} = \chi_{\rm loc} H_{\rm ext}^z \cos\theta$. This magnetization, in turn, has a component $M^z = M^{\shortparallel} \cos\theta = \chi_{\rm loc} H_{\rm ext}^z \cos^2\theta$ along $\hat{\boldsymbol{z}}$, and therefore $\chi_{\rm int} = \chi_{\rm loc} \cos^2\theta$.

To sum up, once the converged $B_i^{\shortparallel}$ and m_i distributions have been determined, N is calculated using Eq. (1),

$$N = \left[\frac{\mu_0 \mu_B}{V B^{\rm ext}} \sum_{i=1}^{\mathcal{N}} m_i \cos\theta\right]^{-1} - \frac{1}{\chi_{\rm loc} \cos^2\theta}. \quad (7)$$

Determination of N via Monte Carlo simulations – With the iterative method we reach system sizes of $\mathcal{O}(10^6)$ spins. However, it is not obvious that this method, which is mean-field like and does not include fluctuations in the m_i's, would give the same result as a full statistical calculation for a given spin Hamiltonian. Therefore, we have also calculated N using Monte Carlo (MC) simulations for a few select physical cases to verify the results of the iterative method. For a single data point, the MC approach requires $\mathcal{O}(10^5)$ core hours [36] to reach the necessary precision for $\mathcal{O}(10^4)$ moments. With the MC method, we cannot set $\chi_{\rm loc}$ as done in the iterative method. Instead, we adjust the temperature, T, in order to tune $\chi_{\rm int}$ to the desired value.

For definitiveness, we use the magnetostatic dipolar Hamiltonian $H = \frac{\mu_0 \mu_B}{4\pi} \sum_{i>j} \Lambda_{ij} \sigma_i \sigma_j$, where $\sigma_i = \pm 1$ and $\Lambda_{ij} = \left[(\hat{\mathbf{i}} \cdot \hat{\mathbf{j}}) - 3(\hat{\mathbf{i}} \cdot \hat{\boldsymbol{r}}_{ij})(\hat{\mathbf{j}} \cdot \hat{\boldsymbol{r}}_{ij})\right] / r_{ij}^3$, and χ^{zz} is determined according to

$$\chi^{zz} = \frac{\partial M^z}{\partial H^z} = \frac{\mu_0 \mu_B}{k_{\rm B} T V} \left\langle \left(\sum_{i=1}^{\mathcal{N}} \sigma_i \cos\theta\right)^2 \right\rangle. \quad (8)$$

Using Ewald boundary conditions we obtain $\chi_{\rm int}^{\rm MC}$, while open boundary conditions yield $\chi_{\rm exp}^{\rm MC}$, and N is obtained from Eq. (1).

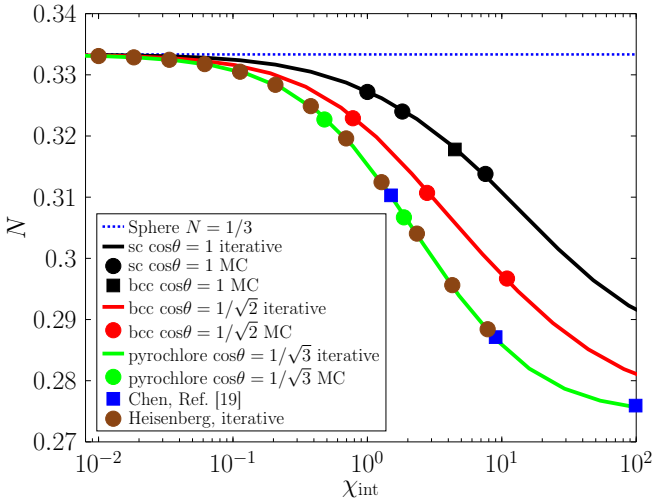

FIG. 2. N as a function of $\chi_{\rm int}$ for cubic samples of various lattices (see main text). The lines are the results of the iterative calculation, while symbols are MC check points. The blue squares are from Chen *et al.* [19]. Maroon circles indicate an iterative calculation for spherically symmetric (Heisenberg) spins on an sc lattice.

Experimental determination of N– We determined N for a cube of $Dy_2Ti_2O_7$ spin ice using $N = 1/\chi_{\rm exp}^{\rm cs} - 1/\chi_{\rm exp}^{\rm ss} + 1/3$, where $\chi_{\rm exp}^{\rm cs}$ and $\chi_{\rm exp}^{\rm ss}$ are the *experimentally measured* susceptibilities of a cubic and a spherical sample respectively. In order to match the level of the susceptibility of the cube and sphere in the high-T limit, $\chi_{\rm exp}^{\rm cs}$ was shifted by about 1% ($\chi_{\rm exp}^{\rm cs} \to \chi_{\rm exp}^{\rm cs}/1.0074$) before calculating N.

The two samples were obtained from different larger crystals provided by D. Prabhakaran [37]. The spherical sample of diameter 4 mm was made by commercial hand-cutting techniques similar to the ones employed in Ref. [23]. The cubic sample, of dimensions $2 \times 2 \times 2$

mm^3, and with all edges precisely oriented with the crystallographic axes a, b, c, was cut and epi-polished on all sides [38]. We carefully controlled the crystal shape and orientation as well as experimental set up to minimize all potential sources of uncertainty and systematic errors in the measurement.

Results – Our main experimental result is shown in Fig. 1, where we display the experimentally determined N as a function of T for the cubic single crystal sample of $Dy_2Ti_2O_7$ spin ice. The main theoretical result is shown in Fig. 2, where N is displayed as a function of $\chi_{\rm int}$ for cubic samples. We have considered the simple cubic (sc) and body centered cubic (bcc) lattices with the Ising direction parallel to $\boldsymbol{B}^{\rm ext}$. We also display results for two lattices with Ising spins tilted away from $\boldsymbol{B}^{\rm ext}$. First, a bcc lattice, with spins pointing in the (101) and (−101) directions. Second, a pyrochlore lattice built from the conventional cubic unit cell [39]. Finally, we include results for the dipolar model with spherically symmetric Heisenberg spins on an sc lattice. Results (not shown) for a tetragonal Ising lattice, relevant to $LiHoF_4$ [40], are found to be identical to the sc case.

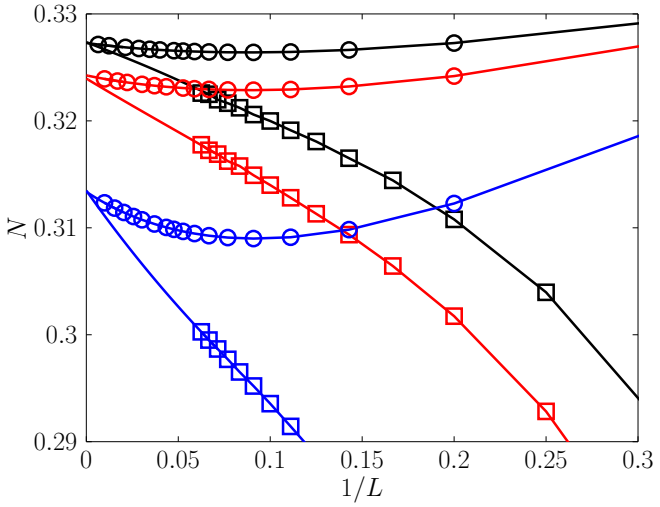

FIG. 3. N as a function of inverse linear system size $1/L$ for a cubic sample of the sc lattice. Shown are $\chi_{\rm int}$=1.00 (black), 1.82 (red) and 7.53 (blue) for the iterative method (circles), and Monte Carlo method (squares).

All results are extrapolated to infinite system size and in Fig. 3 we compare the system-size dependence of the two methods. Extrapolations have been performed using the functional form $a+b/L+c/L^2$ for the iterative demagnetizing factor and $\chi^{\rm MC}_{\rm exp}$, while we used $a+b/L^3+c/L^4$ for $\chi^{\rm MC}_{\rm int}$, where L is the linear system size of the cube [41].

Discussion – The experimental result in Fig. 1 verifies the explicit T dependence of N for a cuboid. Furthermore, the theoretical prediction matches the experimental data well, even though the short-range exchange interaction in $Dy_2Ti_2O_7$ was not included in the simulation [42, 43]. The results in Fig. 2 indicate that N clearly depends on the symmetry and direction of the moments, and that the MC and iterative calculations agree. The sc, bcc and $LiHoF_4$ lattices with Ising spins aligned along $B_{\rm ext}$ yield the same N, indicating that it is not directly sensitive to the specific symmetry of the lattice itself. Turning the local Ising axes away from $B_{\rm ext}$ causes a more rapid decrease of N with increasing $\chi_{\rm int}$. The pyrochlore lattice with tilt angle $\cos\theta = 1/\sqrt{3}$ yields a smaller N than the bcc lattice with $\cos\theta = 1/\sqrt{2}$ for $\chi_{\rm int} > 0$. It is interesting to note that the spin ice pyrochlore lattice yields the same result as the continuum method of Chen *et al.* [19], and the dipolar model with Heisenberg spins. It is therefore tempting to conjecture that models for which χ is independent of the direction of $B_{\rm ext}$ will follow the behavior calculated by Chen *et al.* The L dependence in Fig. 3 shows that the iterative method is asymptotically exact in the limit of large L.

What are the lessons of experimental relevance pertaining to the determination of N? If accurate measurements of $\chi_{\rm int}$ is the objective, then the corrections to $N(\chi\to 0)$ identified here can become very important for $\chi \gtrsim N$. We emphasize that this is not simply a minor quantitative correction, but the effects may be dramatic. For example, in the case of $Dy_2Ti_2O_7$, $T\chi_{\rm int}(T)$ features a peak, which is easily shifted outside the experimental temperature window by application of the ordinary $\chi = 0$) demagnetizing correction [23]. More generally, while the demagnetizing correction can in principal be controlled for highly elongated samples or ellipsoids, it is not always easy to prepare real samples that approximate these idealizations. This is particularly true of non-metallic (and perhaps brittle) samples, which have become of much greater interest in recent years – spin ice [44] and $LiHoF_4$ [40] being well-known examples. Therefore, insofar as cuboids are often the most practical sample shapes to accurately prepare, the best approach may be to use cuboidal samples and apply the theoretical corrections identified here.

In conclusion, considering the demagnetizing problem as a paradigm for the study of effects caused by long-range interactions, our results confirm that N may be precisely defined for cuboidal samples. This implies that the free energy gains a non-additive part of the form $F_{\rm mag} = (\mu_0/2)VN(T)M^2$ in the approach to the thermodynamic limit [45] and that the spatially averaged internal field and magnetisation are conjugate thermodynamic variables. By going beyond Maxwell's continuum theory, we show that N depends not only on the sample shape and χ,but also on microscopic factors: specifically the spin dimensionality and the effective magnetic symmetry of the crystallographic basis. Given that details of the lattice and local environment may affect even such a fundamental and well-studied macroscopic property as N, it is interesting to ask whether microscopic properties could be at play in other systems with long-range inter-

actions. A full understanding of how the thermodynamic limit is reached for long-ranged and conditionally convergent interactions continues to offer challenging problems to theorists and experimentalists alike.

We thank D. Prabhakaran for providing crystals from which the samples were cut, and J. Rau for useful discussions. The simulations were performed on resources provided by the Swedish National Infrastructure for Computing (SNIC) at the Center for High Performance Computing (PDC) at the Royal Institute of Technology (KTH). MT and PH are supported by the Swedish Research Council (2013-03968), MT is grateful for funding from Stiftelsen Olle Engkvist Byggmästare (2014/807), LB is supported by The Leverhulme Trust through the Early Career Fellowship program (ECF2014-284). This research was supported in part by the Perimeter Institute for Theoretical Physics. Research at the Perimeter Institute is supported by the Government of Canada through Innovation, Science and Economic Development Canada and by the Province of Ontario through the Ministry of Research, Innovation and Science. The work at the U. of Waterloo was supported by the Canada Research Chair program (M.G., Tier 1).

[1] A. Campa, T. Dauxois, and S. Ruffo, Phys. Rep. **480**, 57 (2009).
[2] J. A. Osborn, Phys. Rev. **67**, 351 (1945).
[3] E. C. Stoner, Philos. Mag. **36**, 803 (1945).
[4] M. Beleggia, M. De Graef, and Y. T. Millev, Philos. Mag. **86**, 2451 (2006).
[5] M. Beleggia, M. De Graef, and Y. T. Millev, J. Phys. D **39**, 891 (2006).
[6] G. Di Fratta, Proc. R. Soc. A **472**, 0197 (2016).
[7] I. Ponomareva, I. I. Naumov, I. Kornev, H. Fu, and L. Bellaiche, Phys. Rev. B **72**, 140102 (2005).
[8] J. D. Eshelby, Proc. R. Soc. A **241**, 376 (1957).
[9] G. Durin and S. Zapperi, J. Appl. Phys. **87**, 7031 (2000).
[10] F. F. Csikor, C. Motz, D. Weygand, M. Zaiser, and S. Zapperi, Science **318**, 251 (2007).
[11] L. Laurson, X. Illa, S. Santucci, K.-T. Tallakstad, K. J. Måløy, and M. J. Alava, Nat. Comm. **4**, 2927 (2013).
[12] D.-X. Chen, J. A. Brug, and R. B. Goldfarb, IEEE Trans. Magn. **27**, 3601 (1991).
[13] A. Aharoni, J. Appl. Phys. **83**, 3432 (1998).
[14] J. Würschmidt, Z. Phys. **12**, 128 (1923).
[15] F. Stäblein and H. Schlechtweg, Z. Phys. **95**, 630 (1935).
[16] J. A. Quilliam, S. Meng, C. G. A. Mugford, and J. B. Kycia, Phys. Rev. Lett. **101**, 187204 (2008).
[17] R. Higashinaka and Y. Maeno, Phys. Rev. Lett. **95**, 237208 (2005).
[18] D.-X. Chen, E. Pardo, and A. Sanchez, IEEE Trans. Magn. **38**, 1742 (2002).
[19] D.-X. Chen, E. Pardo, and A. Sanchez, IEEE Trans. Magn. **41**, 2077 (2005).
[20] P. H. Christensen and S. Mørup, J. Magn. Magn. Mater. **35**, 130 (1983).
[21] E. Y. Vedmedenko, H. P. Oepen, and J. Kirschner, J. Magn. Magn. Mater. **256**, 237 (2003).
[22] Y. T. Millev, E. Vedmedenko, and H. P. Oepen, J. Phys. D **36**, 2945 (2003).
[23] L. Bovo, L. D. C. Jaubert, P. C. W. Holdsworth, and S. T. Bramwell, J. Phys.: Condens. Matter **25**, 386002 (2013).
[24] C. Castelnovo, R. Moessner, and S. L. Sondhi, Nature **451**, 42 (2008).
[25] A. Biltmo and P. Henelius, Nat. Comm. **3**, 857 (2012).
[26] T. Fennell, S. T. Bramwell, D. F. McMorrow, P. Manuel, and A. R. Wildes, Nat. Phys. **3**, 566 (2007).
[27] J. P. C. Ruff, R. G. Melko, and M. J. P. Gingras, Phys. Rev. Lett. **95**, 097202 (2005).
[28] H. Sato, K. Matsuhira, T. Tayama, Z. Hiroi, S. Takagi, and T. Sakakibara, Journal of Physics: Condensed Matter **18**, L297 (2006).
[29] H. Sato, K. Matsuhira, T. Sakakibara, T. Tayama, Z. Hiroi, and S. Takagi, Journal of Physics: Condensed Matter **19**, 145272 (2007).
[30] P. Schiffer, A. P. Ramirez, D. A. Huse, and A. J. Valentino, Phys. Rev. Lett. **73**, 2500 (1994).
[31] J. A. Quilliam, L. R. Yaraskavitch, H. A. Dabkowska, B. D. Gaulin, and J. B. Kycia, Phys. Rev. B **83**, 094424 (2011).
[32] D. J. Griffiths, *Introduction to Electrodynamics*, 3rd ed. (Prentice-Hall, 1999).
[33] D. J. Griffiths, American Journal of Physics **50**, 698 (1982).
[34] J. D. Jackson, *Classical Electrodynamics*, 2nd ed. (John Wiley & Sons, 1975).
[35] P. P. Ewald, Ann. Phys. **369**, 253 (1921).
[36] Intel Xeon E5-2698v3 processors with Cray Aries interconnect between nodes.
[37] D. Prabhakaran and A. Boothroyd, Crys. Growth **318**, 1053 (2011).
[38] SurfaceNet GmbH, http://www.surfacenet.de.
[39] R. G. Melko and M. J. P. Gingras, J. Phys.: Condens. Matter **16**, R1277 (2004).
[40] M. J. P. Gingras and P. Henelius, J. Phys.: Conf. Ser. **320**, 012001 (2011).
[41] M. E. J. Newman and G. T. Barkema, *Monte Carlo Methods in Statistical Physics*, 1st ed. (Oxford University Press, 1999).
[42] T. Yavors'kii, T. Fennell, M. J. P. Gingras, and S. T. Bramwell, Phys. Rev. Lett. **101**, 037204 (2008).
[43] P. Henelius, T. Lin, M. Enjalran, Z. Hao, J. G. Rau, J. Altosaar, F. Flicker, T. Yavors'kii, and M. J. P. Gingras, Phys. Rev. B **93**, 024402 (2016).
[44] M. J. P. Gingras, "Introduction to frustrated magnetism," (Springer (Ed. Lacroix, Mendels & Mila), 2011) Chap. Spin Ice.
[45] P. Rhodes and G. Rowlands, Proc. Leeds Phil. Lit. Soc. **6**, 191 (1954).